Rapid Communications

Polaritonic frequency-comb generation and breather propagation in a negative-index metamaterial with a cold four-level atomic medium

Saeid Asgarnezhad-Zorgabad,[1,2] Pierre Berini,[3,4,5] and Barry C. Sanders[2,6,*]

[1]*Department of Physics, Sharif University of Technology, Tehran 11365 11155, Iran*
[2]*Institute for Quantum Science and Technology, University of Calgary, Calgary, Alberta, Canada T2N 1N4*
[3]*Department of Physics, University of Ottawa, 150 Louis-Pasteur, Ottawa, Ontario, Canada K1N 6N5*
[4]*Centre for Research in Photonics, University of Ottawa, 25 Templeton St., Ottawa, Ontario, Canada K1N 6N5*
[5]*School of Electrical Engineering and Computer Science, 700 King Edward St., Ottawa, Ontario, Canada K1N 6N5*
[6]*Program in Quantum Information Science, Canadian Institute for Advanced Research, Toronto, Ontario, Canada M5G 1M1*

(Received 15 February 2019; published 10 May 2019)

We develop a concept for a waveguide that exploits spatial control of nonlinear surface-polaritonic waves. Our scheme includes an optical cavity with four-level N-type atoms in a lossless dielectric placed above a negative-index metamaterial layer. We propose exciting a polaritonic Akhmediev breather at a certain position of the interface between the atomic medium and the metamaterial by modifying laser-field intensities and detunings. Furthermore, we propose generating position-dependent polaritonic frequency combs by engineering widths of the electromagnetically induced transparency window commensurate with the surface-polaritonic modulation instability. Therefore, this waveguide acts as a high-speed polaritonic modulator and position-dependent frequency-comb generator, which can be applied to compact photonic chips.

DOI: 10.1103/PhysRevA.99.051802

Nonlinear plasmonics (and polaritonics) [1] in waveguide geometries are of strong interest for schemes enabling strong cross-phase modulation [2], amplification and lasing [3], modulators [4], and detection [5]. Controlling and exciting nonlinear surface polaritons (SPs) is challenging as the strength of the nonlinear processes and their efficiency depend strongly on (metallic) nanostructure roughness [6,7] which is experimentally challenging to minimize. We circumvent this problem by formulating an approach that spatially controls nonlinear SP waves, and we explore its application for modulation [4] and frequency-comb generators [8].

For spatial control of nonlinear surface-polaritonic waves, we suggest driving four-level N-type atoms (4NAs) [9] on the surface of a negative-index metamaterial (NIMM) [10] as depicted in Fig. 1. These components are contained in a stable cavity and serve as a nonlinear planar waveguide. The atoms are dopants in a transparent medium over a thickness of several dipole-transition wavelengths. These atoms are driven by three copropagating fields, a pump signal (s), a weak probe signal (p), and a standing-wave coupling signal (c), all assumed injected from laser beams using the end-fire coupling technique [11,12].

A NIMM can be implemented following one of several approaches [13]. Here we assume a lossless nanofishnet structure, and employ a macroscopic description of the NIMM, which involves an equivalent real permittivity and an equivalent real permeability, following the Drude-Lorentz model [14,15]. We assume that the NIMM is infiltrated with, e.g., a dipolar gain medium such as a dye [10]. This system is pumped either perpendicularly through the bottom or via a guided pump excited by end-fire coupling (not shown) at a wavelength that is off-resonant to the 4NA transitions of interest so that the NIMM becomes lossless for the SP waves of interest. In our scheme, loss compensation is applied independently to the NIMM and does not affect the evolution of the nonlinear SPs. We employ a macroscopic description involving macroscopic permittivity and permeability, which are inserted into the Drude-Lorentz model [14,15].

The use of equivalent macroscopic electromagnetic parameters for the NIMM implies that our scheme can, in principle, be applied to other systems supporting surface waves, such as a metal film supporting loss-compensated surface plasmons [3]. This is further supported by the fact that the NIMM layer can be modeled as an equivalent medium comprising both free-moving electric and (fictitious) magnetic charges [16].

The 4NA is appealing because of its giant Kerr nonlinearity and controllable dispersion [17]. We assume that the signal (s), probe (p), and coupling (c) laser fields drive the $|4\rangle \leftrightarrow |1\rangle$, $|3\rangle \leftrightarrow |1\rangle$, and $|3\rangle \leftrightarrow |2\rangle$ atomic transitions, respectively. The 4NA medium in our waveguide is assumed as Pr^{3+} in Y_2SiO_5 with corresponding energy levels

$$|1\rangle = |^3H_4, \pm 5/2\rangle\,, \quad |2\rangle = |^3H_4, \pm 3/2\rangle\,,$$
$$|3\rangle = |^1D_2, \pm 3/2\rangle\,, \quad |4\rangle = |^1D_2, \pm 5/2\rangle\,. \tag{1}$$

The 4NA medium has atomic density N_a, natural decay rates Γ_{mn}, and dephasing rates $\gamma_{nm}^{\mathrm{dep}}$ for the level transitions $|n\rangle$ and $|m\rangle$ [18]. Inhomogeneous broadening of the transition between levels $|n\rangle$ and $|m\rangle$, W_{nm}, is negligible for a cooled Rb gas due to the Doppler effect being weak, but the effects of inhomogeneous broadening (of the order of gigahertz at

*sandersb@ucalgary.ca;
http://iqst.ca/people/peoplepage.php?id=4

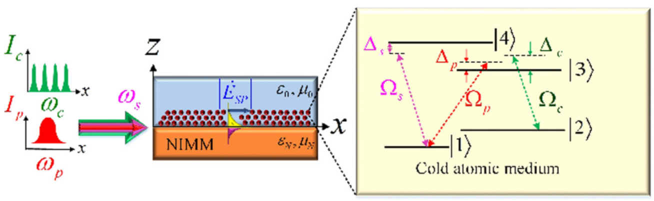

FIG. 1. Our proposed polaritonic waveguide comprises a 4NA medium as a thin doped layer in a lossless dielectric placed above a NIMM half-space. The waveguide is placed in a cavity (not shown) and the 4NA medium driven by three copropagating signals, a pump signal (s), a weak probe signal (p), and a standing-wave coupling signal (c), all assumed injected from laser beams using the end-fire coupling technique. The cavity produces a resonant mode at the coupling frequency only, so this wave is illustrated as a standing wave.

near-liquid-helium temperatures [19]) could be non-negligible for our solid-state medium. Inhomogeneous broadening mechanisms, including dipole-dipole and spin-spin interactions [20] would be relevant, but their inclusion in nonlinear SP dynamics exceeds the scope of our study.

The signal, probe, and coupling laser fields interact with the 4NAs in the waveguide within an optical cavity of length ℓ. The signal detuning frequencies are $\Delta_{\mathrm{s,p,c}}$, and the Rabi frequencies are $\Omega_{\mathrm{s,p,c}}$ with

$$\Omega_{\mathrm{c}}(x) = \Omega_{\mathrm{c}}^{(0)} \sin\frac{x}{\ell} \tag{2}$$

for constant Rabi-frequency coefficient $\Omega_{\mathrm{c}}^{(0)}$ and longitudinal coordinate, or position, x. The fields are evanescently confined to the NIMM-4NA interface with decay functions $\zeta_{\mathrm{c,p,s}}(z)$. The decay functions are maximum at the interface, and we assume that $\zeta_{\mathrm{c}} \equiv \zeta_{\mathrm{s}} \approx \zeta_{\mathrm{p}}$ [21].

We show that these laser driving fields would excite nonlinear SP waves including Akhmediev breathers, which is a solitary localized nonlinear wave with a periodically oscillating amplitude [22], and a frequency comb, as a nonlinear wave that appears briefly at specific positions. We propose generating these nonlinear waves by coupling the probe laser to the dipole moment of the 4NA $|3\rangle \leftrightarrow |1\rangle$ transition, and stability is achieved by imposing an SP low-loss condition and modifying the nonlinearity and dispersion of SPs at the interface.

Our quantitative description of the system is obtained by solving Maxwell-Bloch equations [23] based on a perturbative, asymptotic, multiscale position (x) and time (t) expansion [24]

$$x_l = \varepsilon^l x, \quad t_l = \varepsilon^l t, \quad \varepsilon := \max\left\{\left|\frac{\Omega_{\mathrm{p}}}{\Omega_{\mathrm{c}}}\right|, \left|\frac{\Omega_{\mathrm{p}}}{\Omega_{\mathrm{s}}}\right|\right\}, \tag{3}$$

for ε the perturbation scale coefficient. Our third-order truncated solution yields a nonlinear Schrödinger equation (NLSE). We solve and plot the Rabi frequency for the resultant surface-polaritonic Akhmediev breather and explore Rabi-frequency dependence as a function of various control parameters to identify conditions for efficient frequency-comb generation.

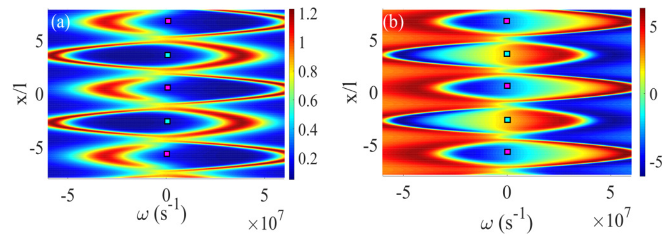

FIG. 2. (a) Asymmetric absorption and (b) dispersion spectra of the linear SPs. Magenta dots ($x_j^{(\mathrm{a})}$) represent the position for which time-periodic nonlinear waves with maximum amplitude are generated. Blue dots ($x_j^{(\mathrm{f})}$) show positions for efficient polaritonic frequency-comb generation.

We use only $x_{0,1,2}$ and $t_{0,1}$ in our analysis by ignoring three effects, namely, (i) the second-order x_1 derivative due to a slowly varying amplitude [25], (ii) higher-order timescales $t_{l>1}$ and position $x_{l>2}$, in deriving Eq. (6) by ignoring higher-order dispersion, and (iii) group-velocity dispersion (GVD) in the NIMM layer, which is 10^{-5} times the 4NA GVD.

We treat SPs as plane waves with GVD $K_2(\omega, x) := \partial^2 K(\omega, x)/\partial\omega^2$ for $K(\omega, x)$ the linear dispersion. The SP absorption coefficient is $\bar{\alpha} := \varepsilon^2 \mathrm{Im}[K(\omega, x)]$, and we neglect GVD and self-phase modulation (SPM) (W) variability at different orders of position scales: $\mathcal{J}(x_l, \omega)$ is constant for all l for $\mathcal{J} \in \{K, K_2, W\}$. Nonlinear SPs have large initial pulse width τ_{p}, group velocity $v_{\mathrm{g}} = [\partial K(\omega, x)/\partial\omega]^{-1}$, and half-Rabi frequency

$$U_0 = \sqrt{\frac{K_{2\mathrm{av}}}{\tau_{\mathrm{p}}^2 W_{\mathrm{av}}}}, \tag{4a}$$

$$K_{2\mathrm{av}} = \int_{-\ell/2}^{\ell/2} dx\, K_2(x), \quad W_{\mathrm{av}} = \int_{-\ell/2}^{\ell/2} dx\, W(x), \tag{4b}$$

and propagate up to several nonlinear units of length given by $L_{\mathrm{N}} = 1/(U_0^2|W|)$ if the imaginary parts of the GVD and SPM are much smaller than the real parts.

We replace

$$t - \frac{x}{v_{\mathrm{g}}} \mapsto \sigma := \frac{\tau}{\tau_{\mathrm{p}}}, \quad x \mapsto s := \frac{x}{L_{\mathrm{N}}}, \tag{5}$$

ignoring the atomic absorption due to an electromagnetically induced transparency (EIT) window. We normalized GVD and SPM according to $g_\iota(x) = \mathcal{J}(x)/\mathcal{J}_{\mathrm{av}}$. Dynamics of the normalized SP pulse envelope $u = [\Omega_{\mathrm{p}}/U_0]\exp(-\alpha x)$ follows

$$i\frac{\partial u}{\partial s} - \frac{g_{\mathrm{D}}(x)}{2}\frac{\partial^2 u}{\partial\sigma^2} - g_{\mathrm{N}}(x)|u|^2 u \approx 0, \tag{6}$$

which is a dimensionless NLSE [26]. Our nonlinear Schrödinger equation matches the equation in earlier work that exhibits similar GVD and SPM [24], but our results differ from previous work due to dissimilar broadening mechanisms in the the two systems.

We propose employing the spatially modulated coupling laser for SP absorption-dispersion control during its propagation, which we illustrate by plotting SP absorption and dispersion in Figs. 2(a) and 2(b), respectively. Asymmetric absorption-dispersion profiles for the position-dependent SPs are evident, and we see the formation of multiple static EIT windows in the propagation direction by coupling laser modulation. We reduce atomic absorption by adjusting the spatially modulated control field and other laser field intensities for the wavelength corresponding to the $|3\rangle \leftrightarrow |1\rangle$ atomic transition (i.e., for $\omega \approx 0$). Therefore, points in the propagation direction correspond to $\omega = 0$ for the multiple EIT windows seen in Figs. 2(a) and 2(b). These EIT windows are suitable for propagating nonlinear polaritonic waves including Akhmediev breathers and frequency combs.

We choose realistic parameters to analyze the performance of this polaritonic waveguide [27]. Radiative decay is quantified by $\Gamma_{31}^{\mathrm{R}} = \Gamma_{43} = 9$ kHz and nonradiative decay by $\Gamma_{31}^{\mathrm{NR}} \approx 6$ kHz. The atomic density is $N_{\mathrm{a}} = 4.7 \times 10^{18}\ \mathrm{cm}^{-3}$, and we propose using a R6G ring dye laser as input sources with $\lambda_l \approx 606$ nm, $\Omega_{\mathrm{s}} = 28$ MHz, $\Omega_{\mathrm{c}}^{(0)} = 80$ MHz, $\Delta_{\mathrm{s}} = 0.07$ MHz, $\Delta_{\mathrm{c}} = 0.2$ MHz, and $\Delta_{\mathrm{p}} = 0$. Realistic parameters are also employed for the NIMM layer [10,28]. Inhomogeneous broadening effects in the transitions $\{W_{nm}\}$ of Pr^{3+} levels on the nonlinear evolution of the SPs are neglected in our model but could be incorporated by selecting homogeneously broadened subensembles of Pr ions selected by spectral hole burning [29].

We suggest two sets of positions corresponding to $\omega \approx 0$ for stable propagation of nonlinear polaritonic waves including Akhmediev breathers and frequency combs. (i) At positions

$$x_j^{(\mathrm{a})} = (-5.68 + 2j\pi)\ell, \quad j \in \{0, 1, \dots\}, \tag{7}$$

nonlinear SPs propagate with $v_{\mathrm{g}} \approx 2.91 \times 10^{-2}$c within $\Delta x \approx \ell/2$, and

$$K_2 = (1.45 + 0.09i) \times 10^{-15}\ \mathrm{cm}^{-1}\,\mathrm{s}^2, \tag{8a}$$

$$W = (-1.47 + 0.11i) \times 10^{-15}\ \mathrm{cm}^{-1}\,\mathrm{s}^2, \tag{8b}$$

respectively, are constant with $g_{\mathrm{D}}(x) \approx g_{\mathrm{N}} \approx -1.01$. Therefore, at these specific positions SPs propagate as polaritonic Akhmediev breathers. (ii) For

$$x_j^{(\mathrm{f})} = (-2.61 + 2j\pi)\ell, \tag{9}$$

GVD and SPM are position dependent within $\Delta x \approx \ell/2$ so

$$K_{2\mathrm{av}} = (5.87 + 0.25i) \times 10^{-18}\ \mathrm{cm}^{-1}\,\mathrm{s}^2, \tag{10a}$$

$$W_{\mathrm{av}} = (-1.01 + 0.04i) \times 10^{-15}\ \mathrm{cm}^{-1}\,\mathrm{s}^2. \tag{10b}$$

At these points, SPs propagate with weak dispersion and strong nonlinearity as efficient polaritonic-frequency combs.

Exploiting the correspondence between energy levels of the Bogoliubov spectrum ($E_{\pm l}$) of the uniform Bose gas with kinetic energy (Δk) [30] and energy transference between nonlinear polaritonic modes in EIT windows, we propose generating polaritonic sidebands with modulation frequency Ω and growth rate b and thereby realize Akhmediev breather excitation. Our analysis shows energy transfer from the zeroth-order ($l = 0$) polaritonic wave with propagation constant b', $\Omega_{\mathrm{p}}^0(x) = \exp(ib'\tilde{x})$, to the first-order sidebands ($l = \pm 1$) by setting $\Delta k = \Omega$ and $E_{\pm 1} = b$.

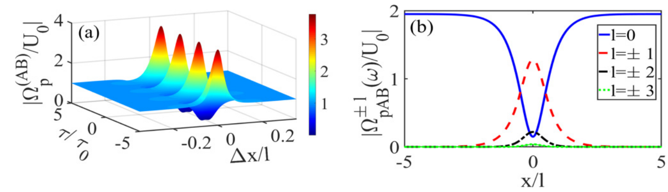

FIG. 3. Panel (a) represents the GVD-SPM modulation and stable propagation of the polaritonic Akhmediev breather for Δx. Panel (b) represents the energy transfer to other polaritonic sidebands. The parameters for this simulation are $\Omega = \sqrt{3}/2$ and $\delta\phi = 0.1\pi$ and the other parameters are given in the text.

We thereby obtain the wave with amplification factor $b = -ib'$ according to

$$\Omega_{\mathrm{p}}^{\pm 1}(x) = e^{b\tilde{x}}, \quad \tilde{x} := x\left[K(\omega) + \frac{1}{2L_{\mathrm{N}}}\right]. \tag{11}$$

Energy transmittance to third-order polaritonic sidebands ($l = \pm 3$) is depicted in Fig. 3(b) and is in accordance with energy conservation

$$\left|\Omega_{\mathrm{p}}^0\right|^2 + 2\sum_{|l|>1}\left|\Omega_{\mathrm{p}}^{\pm l}(x)\right|^2 = 1. \tag{12}$$

In our scheme, a stable polaritonic Akhmediev breather propagates for $\alpha \approx 0.25$, $\Omega = 0.8$, and $b = 0.73$ within $\Delta x = \ell/2$ within EIT windows such that $\delta\omega_{\mathrm{EIT}} \approx 30$ MHz as shown in Fig. 3(a).

Our waveguide serves as a fast-phase modulator [31] according to stable polaritonic-breather propagation. To this aim, we rewrite the surface-polaritonic Akhmediev breather solution as $\Omega_{\mathrm{p}}^{\mathrm{AB}} = |\Omega_{\mathrm{p}}^{\mathrm{AB}}| \exp[i \arg(\Omega_{\mathrm{p}}^{\mathrm{AB}})]$. For our realistic parameters, $\arg(\Omega_{\mathrm{p}}^{\mathrm{AB}}) \approx \pi$ which is the phase shift between initial and recovered plane SP waves after breather formation. Nonlinear pulses are compressed typically to several picoseconds in telecommunication fiber [32]. As our proposed 4NA-NIMM structure has high nonlinear dispersion, including large SPM, significant compression beyond the scale of what is achieved in fiber is expected due to growth-return evolution ($\delta t = 12$ ps). Significant pulse compression beyond the scale of an optical fiber is expected. Highly compressed pulses are useful in fast all-optical switching applications.

We propose efficient polaritonic-frequency combs by rewriting

$$g_\iota(x) = g_\iota^{\mathrm{c}} + g_\iota^{\mathrm{p}}(x), \quad \iota \in \{D, N\} \tag{13}$$

in terms of constant and position-dependent parts. The frequency combs can be excited at specific positions $x_j^{(\mathrm{f})}$, where nonlinear SPs exhibit low GVD [$|g_{\mathrm{D}}^{\mathrm{p}}(x)| \ll 1$] and strong nonlinearity [$|g_{\mathrm{N}}^{\mathrm{p}}(x)| \approx 1$]. Therefore, we neglect GVD and replace $g_{\mathrm{D}}[\partial^2 u/\partial\sigma^2] \mapsto 0$ (6) and assume $g_{\mathrm{N}}^{\mathrm{c}} \approx -1$. The resultant expression admits an initial SP wave with input power P_0 of the form

$$u(x) = \sqrt{P_0}\exp\left[-iP_0\int dx' g_{\mathrm{N}}(x')\right]. \tag{14}$$

We claim that stable propagation of nonlinear SPs in the weak-dispersion limit depends on the EIT-window widths and the normalized nonlinear coefficient $g_{\mathrm{N}}^{\mathrm{p}}(x)$.

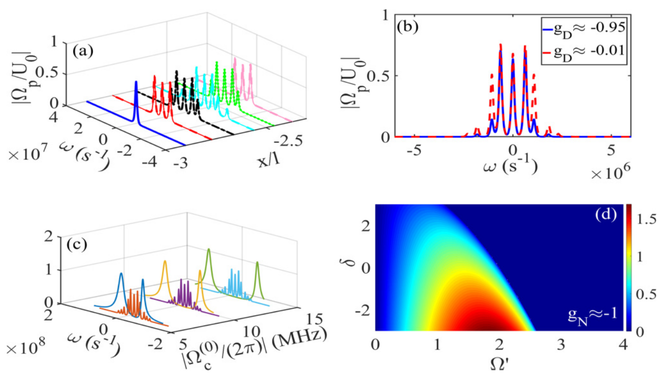

FIG. 4. Panel (a) represents the propagation of the plane SP waves around the $x_0^{(f)}$ dots. (b) Comparison of the Akhmediev breather $g_D = -0.95$ and efficient frequency combs $g_D \approx 0.01$. In panel (c) we apply different $\Omega_c^{(0)}$ to achieve efficient frequency combs and panel (d) represents the gain map of the polaritonic modulation instability.

We propose efficient surface-polaritonic frequency combs by SP propagation along the interface shown in Fig. 3(a) with $\delta\phi = 0.1\pi$, $P_0 \approx 10\ \mu$W. Then we numerically solve the NLSE together with initial condition (14) within $-3\ell < x_0^{(f)} < -2.5\ell$. We obtain a modulated EIT window, strong nonlinearity, and consequently efficient polaritonic frequency combs. Specifically, for $x_0^{(f)}$ with $\delta\omega_{\rm EIT} = 25$ MHz and $g_D \approx 0.01$, frequency combs up to $\delta\omega_{\rm comb} \approx 11.2$ MHz with stability $|\Omega_p(x)| \approx 0.87|\Omega_p(x=0)|$ are excited. However, outside the EIT window, the generated polaritonic combs are highly unstable due to high atomic absorption.

This model allows us to develop a condition to generate efficient surface-polaritonic frequency combs via position-dependent GVD and SPM. To this aim, we consider $\Delta x = x_* = \varepsilon$ as a small propagation length and add a perturbative term to Eq. (14) of the form

$$u(x,t) = \{\sqrt{P_0} + \varepsilon p(x) e^{i\omega\tau/\tau_p}\} \times \exp\left[-iP_0 \int_{-\ell/2}^{\ell/2} dx' g_N(x')\right]. \qquad (15)$$

We also expand the SP-wave perturbation frequency around the EIT-window center (ω_*) as a function of the relative polaritonic frequency-comb mode number (ν) in the presence of SPs dispersion

$$\omega = \omega_* + \mathcal{K}_1(x)\nu + \frac{\mathcal{K}_2(x)}{2}\nu^2 + \cdots \qquad (16)$$

with $\{\mathcal{K}_{l>2}\}$ related to higher-order dispersion. Efficient frequency combs are generated by suppressing higher-order dispersion (16); i.e., $|\mathcal{K}_2(x)| \ll c|\mathcal{K}_1(x)|^2$. Specifically, at $x_0^{(a)}$, $\mathcal{K}_1 \approx 0.35$, $\mathcal{K}_2 \approx 2.16 \times 10^{-10}$, and $|\mathcal{K}_2/(c\mathcal{K}_1^2)| \sim 10^{-18} \ll 1$, which yields efficient polaritonic-frequency combs as shown in Fig. 4(a). These efficient polaritonic frequency combs are localized over a short spatial extent, approximately half of the nonlinear propagation length.

We vary the coupling-laser intensity for experimental control of EIT-window widths, leading to efficient polaritonic frequency combs shown clearly for $g_D = 0$ and $\delta\phi = 0.1\pi$ with initial condition (15) solving the NLSE numerically around $x_0^{(f)}$. The number of frequency combs increases by modulating coupling-laser intensity and by engineering the EIT-window widths shown in Fig. 4(c). Comparing our frequency combs to a polaritonic Akhmediev breather reveals that nonlinear waves generated at our proposed position are more efficient than frequency combs excited by Akhmediev breathers, as seen in Fig. 4(b).

We describe the excitation of nonlinear surface-polaritonic waves including a polaritonic Akhmediev breather and frequency combs by employing the concept of pass-band polaritonic modulation instability. We assume the initial SPs with dispersion length $L_D \approx L_N$ according to

$$u(x,t) = u_0 e^{i(k+K(\omega)+1/2L_D)x + i\omega\tau/\tau_p}, \qquad (17)$$

with

$$k = g_{{\rm avi}}|u_0|^2 e^{2{\rm Im}[K(\omega)]x} - \frac{\omega^2}{2} - K(\omega) - \frac{1}{2L_N}. \qquad (18)$$

Moreover, we assume Ω' as a modulation frequency, $\delta = (\omega_* - \omega)/\omega_*$ as the normalized perturbed frequencies, and κ as a modulation parameter in the propagation direction. We have perturbed the SP waves in terms of $p(x), q(x) \ll 1$ as

$$u(x,t) = u_0[1 + p(x)e^{-i\Omega'(\kappa\tilde{x}-\tau)} + q^*(x)e^{i\Omega'(\kappa^*\tilde{x}-\tau)}]. \qquad (19)$$

We also expand the SPs linear dispersion and the nonlinear coefficient as a power series of the normalized perturbation frequency

$$K(\delta) = K_0 + K_1\delta + \frac{K_2}{2}\delta^2 + \mathcal{O}(\delta^3), \quad g_N \approx g_{0N} + g_{N1}\delta, \qquad (20)$$

and linearize the NLSE using Eq. (19) in the weak perturbation limit [33]. The perturbed-wave dispersion relation is

$$\left[\kappa + \tilde{K}_0 + (K_1 - 1)\delta + \frac{K_2}{2}\delta^2\right]^2 + (g_{0N} + g_{N1}\delta)|u_0|^2 - \frac{\Omega'^2}{4} = 0, \qquad (21)$$

with $\tilde{K}_0 = K_0 + 1/2L_N$. The gain map for the perturbed-polaritonic waves, shown in Fig. 4(d), demonstrates that nonlinear-polaritonic waves are excited in EIT windows with $|\delta| < \delta_{\rm EIT}$ and $0.5 < \Omega' < 1$ corresponding to pass-band polaritonic modulation instability.

In summary, we introduce a waveguide that exploits spatial control to excite nonlinear-polaritonic waves including Akhmediev breathers and frequency combs as specific cases. We propose a stable cavity comprising 4NAs in a lossless dielectric above the NIMM layer, on which SPs propagate. The 4NA medium is driven by three copropagating signals, a pump signal (s), a weak probe signal (p), and a standing-wave coupling signal (c), all assumed injected from laser beams using the end-fire coupling technique. We propose stable excitation of polaritonic Akhmediev breathers and energy transfer to other polaritonic sidebands at a certain position of the NIMM-4NA interface by modifying laser-field intensities and detunings through GVD-SPM modulation. Moreover, we demonstrate efficient polaritonic frequency-comb generation at a specified position of the waveguide by engineering EIT-window widths and decreasing GVD commensurate with pass-band regime for polaritonic modulation instability. Modeling the effects of inhomogeneous broadening of Pr^{3+} transitions on the SPM and GVD in our system is challenging and needs further consideration. Our predicted nonlinear waves could be achieved in a specific subensemble of Pr^{3+} atoms, such as occurs under persistent spectral-hole burning. Our proposed waveguide has been analyzed for experimentally feasible conditions and should act as a high-speed polaritonic phase modulator and efficient frequency-comb generator.

This project has been partially supported by NSERC funding.

[1] M. Kauranen and A. V. Zayats, Nat. Photonics **6**, 737 (2012).

[2] S. A. Moiseev, A. A. Kamli, and B. C. Sanders, Phys. Rev. A **81**, 033839 (2010).

[3] P. Berini and I. De Leon, Nat. Photonics **6**, 16 (2012).

[4] J. A. Schuller, E. S. Barnard, W. Cai, Y. C. Jun, J. S. White, and M. L. Brongersma, Nat. Mater. **9**, 193 (2010).

[5] M. L. Brongersma, N. J. Halas, and P. Nordlander, Nat. Nanotechnol. **10**, 25 (2015).

[6] A. Nahata, R. A. Linke, T. Ishi, and K. Ohashi, Opt. Lett. **28**, 423 (2003).

[7] N. Feth, S. Linden, M. Klein, M. Decker, F. Niesler, Y. Zeng, W. Hoyer, J. Liu, S. Koch, J. Moloney *et al.*, Opt. Lett. **33**, 1975 (2008).

[8] X. T. Geng, B. J. Chun, J. H. Seo, K. Seo, H. Yoon, D.-E. Kim, Y.-J. Kim, and S. Kim, Nat. Commun. **7**, 10685 (2016).

[9] J. Sheng, X. Yang, U. Khadka, and M. Xiao, Opt. Express **19**, 17059 (2011).

[10] S. Xiao, V. P. Drachev, A. V. Kildishev, X. Ni, U. K. Chettiar, H.-K. Yuan, and V. M. Shalaev, Nature (London) **466**, 735 (2010).

[11] G. Stegeman, R. Wallis, and A. Maradudin, Opt. Lett. **8**, 386 (1983).

[12] P. Berini, Phys. Rev. B **61**, 10484 (2000).

[13] V. M. Shalaev, Nat. Photonics **1**, 41 (2007).

[14] A. Kamli, S. A. Moiseev, and B. C. Sanders, Phys. Rev. Lett. **101**, 263601 (2008).

[15] S. Xiao, U. K. Chettiar, A. V. Kildishev, V. P. Drachev, and V. M. Shalaev, Opt. Lett. **34**, 3478 (2009).

[16] N. Sang-Nourpour, B. R. Lavoie, R. Kheradmand, M. Rezaei, and B. C. Sanders, J. Opt. **19**, 125004 (2017).

[17] J. Sheng, X. Yang, H. Wu, and M. Xiao, Phys. Rev. A **84**, 053820 (2011).

[18] R. W. Boyd, *Nonlinear Optics*, 3rd ed. (Elsevier, New York, 2003).

[19] A. V. Turukhin, V. S. Sudarshanam, M. S. Shahriar, J. A. Musser, B. S. Ham, and P. R. Hemmer, Phys. Rev. Lett. **88**, 023602 (2001).

[20] E. Kuznetsova, O. Kocharovskaya, P. Hemmer, and M. O. Scully, Phys. Rev. A **66**, 063802 (2002).

[21] C. Tan and G. Huang, Phys. Rev. A **91**, 023803 (2015).

[22] N. Akhmediev and V. Korneev, Theor. Math. Phys. **69**, 1089 (1986).

[23] B. Kraus, W. Tittel, N. Gisin, M. Nilsson, S. Kröll, and J. I. Cirac, Phys. Rev. A **73**, 020302(R) (2006).

[24] S. Asgarnezhad-Zorgabad, R. Sadighi-Bonabi, and B. C. Sanders, Phys. Rev. A **98**, 013825 (2018).

[25] A. R. Davoyan, I. V. Shadrivov, and Y. S. Kivshar, Opt. Express **17**, 21732 (2009).

[26] M. Conforti, S. Li, G. Biondini, and S. Trillo, Opt. Lett. **43**, 5291 (2018).

[27] H.-H. Wang, A.-J. Li, D.-M. Du, Y.-F. Fan, L. Wang, Z.-H. Kang, Y. Jiang, J.-H. Wu, and J.-Y. Gao, Appl. Phys. Lett. **93**, 221112 (2008).

[28] A. A. Kamli, S. A. Moiseev, and B. C. Sanders, Int. J. Quantum Inf. **09**, 263 (2011).

[29] B. Ham, M. Shahriar, and P. Hemmer, Opt. Lett **22**, 1138 (1997).

[30] N. N. Bogoliubov, Izv. Akad. Nauk Ser. Fiz. **11**, 77 (1947) [J. Phys. (USSR) **11**, 23 (1947)].

[31] A. Melikyan, L. Alloatti, A. Muslija, D. Hillerkuss, P. C. Schindler, J. Li, R. Palmer, D. Korn, S. Muehlbrandt, D. Van Thourhout *et al.*, Nat. Photonics **8**, 229 (2014).

[32] K. Hammani, B. Kibler, C. Finot, P. Morin, J. Fatome, J. M. Dudley, and G. Millot, Opt. Lett. **36**, 112 (2011).

[33] S. Chen, F. Baronio, J. M. Soto-Crespo, P. Grelu, and D. Mihalache, J. Phys. A **50**, 463001 (2017).